# Journal of Materials Chemistry A

Accepted Manuscript


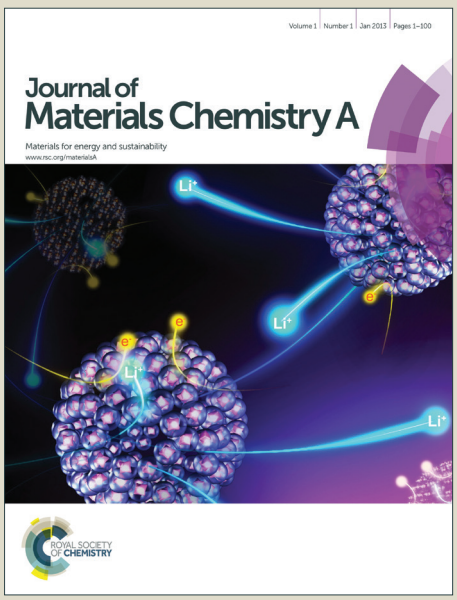





ROYAL SOCIETY OF CHEMISTRY

www.rsc.org/materialsA

Tavorite-type $LiFeSO_4F$ is used to demonstrate the inherent moisture sensitivity issue of sulfate-based materials for Li-ion batteries.

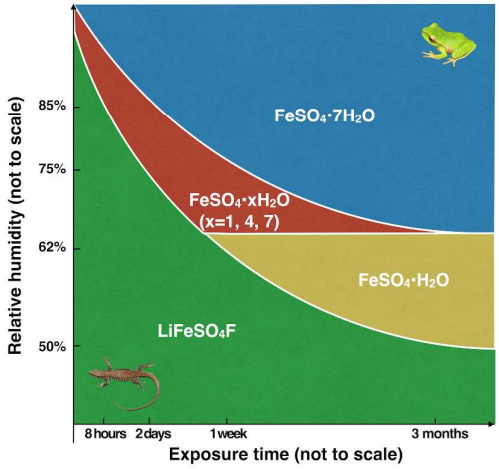

Journal of
Materials Chemistry A

PAPER

# Influence of relative humidity on structure and electrochemical performance of sustainable $LiFeSO_4F$ electrodes for Li-ion batteries†

Received 00th January 2015,
Accepted 00th January 2015

DOI: 10.1039/x0xx00000x

www.rsc.org/

Leiting Zhang[a,b], Jean-Marie Tarascon[*b,c,d], Moulay Tahar Sougrati[d,e], Gwenaëlle Rousse[b,d,f], and Guohua Chen[*a]

Material abundance and eco-efficient synthetic protocols are becoming the overriding factors for developing sustainable Li-ion batteries, hence today's great interest in $LiFePO_4$. The recently reported tavorite-type $LiFeSO_4F$ cathode material, which shows a redox potential of 3.6 V and a practical capacity of ~130 mAh $g^{-1}$ without the need for sophisticated carbon coating or particle downsizing, stands presently as a serious contender to $LiFePO_4$. However, its synthesis is still not routinely reproducible. Herein, we offer a direct explanation by showing the strong effect of the room temperature relative humidity on both $LiFeSO_4F$ aging stability and electrochemical performances. We demonstrate the complete degradation of tavorite-type $LiFeSO_4F$ into $FeSO_4{\cdot}nH_2O$ (n = 1, 4, 7) and LiF in environments with relative humidities greater than 62%, and also show the feasibility of triggering *in situ* formation of a $F^-$-free (Li)$FeSO_4OH$ phase within the cell. This work, which we also extend to the 3.9 V triplite-type $LiFeSO_4F$ polymorph, provides a foundation for achieving the consistent production and handling of $LiFeSO_4F$ electrodes in view of large-scale manufacturing. This moisture sensitivity issue, which can be mitigated by surface treatments, is inherent to sulfate-based electrode materials and the battery community must be aware of it.

## Introduction

Commercialized by Sony in 1990, Li-ion batteries have transformed the global market for portable electronics. However, there is still an appreciable gap for Li-ion batteries to replace gasoline and conquer the automobile industry. Hence, research towards high energy density batteries with environmentally benign and inexpensive electrode materials has been urgently pursued. Today's layered $LiCoO_2$ and its derivative $Li(Ni_{1/3}Mn_{1/3}Co_{1/3})O_2$, termed Li-NMC, are the industry leading positive electrode materials for most electronic gadgets because they offer the highest energy density; however, in large volume electric vehicle (EV) or grid applications, the implementation of these cathode materials will be hindered by materials abundance issues. The polyanionic compound $LiFePO_4$ has received unprecedented attention as an alternative to layered oxide electrodes, and is becoming the most praised material for powering the next generation EVs because it provides safety, cost, and material abundance advantages.

However, due to its low voltage redox potential (3.45 V), the energy density of $LiFePO_4$ cannot fully satisfy the requirement of energy-demanding applications. To partially alleviate this issue and enhance the potential of the $Fe^{3+}/Fe^{2+}$ redox couple, researchers successfully investigated the joint effect of adding electronegative $F^-$ and replacing $PO_4^{3-}$ by a more electronegative sulfate polyanion $SO_4^{2-}$ to prepare a new $LiFeSO_4F$ phase. This phase shows polymorphism; depending on the synthesis conditions $LiFeSO_4F$ crystallizes either in the tavorite or triplite structures, showing redox potentials of 3.6 and 3.9 V for the $Fe^{3+}/Fe^{2+}$ redox couple, respectively.[1-4] Because of these elevated redox voltages, $LiFeSO_4F$ can rival $LiFePO_4$.

The tavorite $LiFeSO_4F$ phase was synthesized by reacting $FeSO_4{\cdot}H_2O$ with LiF via a topotactic reaction ***(Eq. 1)***. Such a reaction, which preserves the structural framework of $FeSO_4{\cdot}H_2O$, enlists the replacement of the water molecules by fluorine and the concomitant ingress of $Li^+$ in the open cavities to preserve electroneutrality.

$$FeSO_4 \cdot H_2O + LiF \rightarrow LiFeSO_4F + H_2O \quad (1)$$

Since the compound is soluble in water, several water-free synthesis protocols have been reported, including solid-state,[5] solvothermal,[6,7] ionothermal,[1] and so forth. Among them the ionothermal process based on the use of 1-ethyl-3-methylimidazolium bis(trifluoromethylsulfonyl)imide (EMI-TFSI) is so far the best option to reproducibly synthesize tavorite $LiFeSO_4F$ with a reversible capacity approaching 140 mAh $g^{-1}$ at a current density of C/10 (charge or discharge 1 $Li^+$ in 10 hours). In the presence of ionic liquids, the water departure from $FeSO_4{\cdot}H_2O$ is postponed by the hydrophobic ionic liquid so as to cope with dissociation kinetics of LiF for enabling the proper reactivity rate of both $F^-$ and $Li^+$ species with the precursor phase. To combat the high cost of ionic liquids, a solvothermal alternative was proposed that consists of using tetraethylene glycol (TTEG) as the solvent. It is

[a] *Department of Chemical and Biomolecular Engineering, The Hong Kong University of Science and Technology, Clear Water Bay, Kowloon, Hong Kong*
[b] *Chimie du Solide et de l'Energie, FRE 3677, Collège de France, 11 place Marcelin Berthelot, 75231 Paris Cedex 05, France*
[c] *Institute for Advanced Study, Visiting Professor of the Department of Chemical and Biomolecular Engineering, The Hong Kong University of Science and Technology, Clear Water Bay, Kowloon, Hong Kong*
[d] *Réseau sur le Stockage Electrochimique de l'Energie (RS2E), FR CNRS 3459, 80039 Amiens, France*
[e] *Institut Charles Gerhardt, CNRS UMR 5253, Université Montpellier 2, 34 095 Montpellier, France*
[f] *UPMC Univ Paris 06, Sorbonne Universités, 4 place Jussieu, F-75005 Paris, France*
[*] *E-mail: jean-marie.tarascon@college-de-france.fr, kechengh@ust.hk*
† Electronic Supplementary Information (ESI) available: SEM images of LiF, XRD patterns of humidity test, electrochemical performances of $FeSO_4{\cdot}H_2O$, water content alaysis, and Mössbauer spectroscopy fittings of aged $LiFeSO_4F$-C. See DOI: 10.1039/x0xx00000x

believed that using hydrophilic TTEG, in contrast to hydrophobic ionic liquid, can help improve the solubility of LiF at elevated temperatures, which is key to the success of the reaction.[6] The tavorite $LiFeSO_4F$ powders synthesized at 220°C *via* the easily scalable TTEG approach were shown to deliver a reversible capacity of 130 mAh $g^{-1}$ at C/10 current density, which is lower than the 140 mAh $g^{-1}$ obtained by the ionothermal route. Although other solvothermal synthetic approaches of $LiFeSO_4F$ were also reported, observed electrode performances were rather inconsistent, indicative of a missing link hindering mastery of the synthesis of this fluorosulfate.[8,9]

Previously, Ati and co-workers noticed the retro-conversion from $LiFeSO_4F$ to $FeSO_4{\cdot}H_2O$ and LiF when trace amount of water was present in organic solvents when assembling batteries,[5] but no detailed mechanism was provided. This phase instability reminds us of another member of the fluorosulfate family, $LiZnSO_4F$, which rapidly decomposes into $ZnSO_4{\cdot}H_2O$ and LiF in open environment. Both of these examples are pointing towards limited stability of these phases towards water. Moreover, sulfate-based electrode materials have long been criticized for their low moisture resistivity in general,[10,11] but comprehensive understanding towards the structural evolution, and more importantly the corresponding changes in electrochemical performance have not been revealed. Thus, we decided to embark on a detailed study of the moisture effect on the synthesis, handling, and performances of tavorite $LiFeSO_4F$. Herein, we report the structural and electrochemical behaviors of $LiFeSO_4F$ to be strongly dependent upon the room temperature relative humidity (RH), namely an increasing deterioration with increasing RH, and demonstrate that this finding can be generalized to other attractive sulfate-based electrodes whether they contain Li or Na as guest species. Through this study we also provide evidence for the electrochemically-driven *in situ* formation of the already reported tavorite-type $(Li)FeSO_4OH$ phase.

## Synthesis and characterization

Equimolar amounts of $FeSO_4{\cdot}H_2O$ and LiF precursors were used to prepare tavorite $LiFeSO_4F$. Owing to both the extremely low solubility of LiF in organic solvents and the large particle size of commercial LiF powders (~10 μm), we decided to synthesize LiF powders *via* a precipitation method. NaF (Riedel-de Haën, 99%) and $LiOH{\cdot}H_2O$ (Sigma-Aldrich, 98%) solutions were used to precipitate LiF. The white powders were characterized by X-ray diffraction (XRD) for phase purity and by scanning electron microscopy (SEM) for morphology. The precipitates were single-phased LiF, as deduced from XRD data recorded from a Philips PW1830 powder X-ray diffractometer (Almelo, Netherlands) equipped with a Cu $K_\alpha$ radiation source ($\lambda = 1.5406$ Å) and a graphite monochromator. From SEM data collected using a JEOL JEM 6700F field-emission scanning electron microscope (Tokyo, Japan) equipped with a cold emission gun and an energy-dispersive X-ray spectrometer, we could deduce that our LiF powders consist of ~1 μm diameter particles as compared to 5-10 μm for commercial LiF (**Fig. S1** Electronic Supplementary Information). Therefore, owing to its highly divided character, this homemade LiF was adopted as the source of Li and F in the following synthesis.

Equally, owing to the importance of having Fe-based precursors free of $Fe^{3+}$ we synthesized our monohydrate $FeSO_4{\cdot}H_2O$ precursor following a routine protocol reported elsewhere.[5] Commercial $FeSO_4{\cdot}7H_2O$ (Sigma-Aldrich, 99%) powders were re-precipitated in water-ethanol with the presence of ascorbic acid to remove $Fe^{3+}$ ions. The recuperated powders were immersed in excess amount of ionic liquid EMI-TFSI ($C_8H_{11}F_6N_3O_4S_2$, Shanghai Chengjie, >98%) and the temperature was slowly increased to and maintained at 100 ˚C for 2 hours to allow the formation of $FeSO_4{\cdot}H_2O$. The recovered white powders were identified as pure $FeSO_4{\cdot}H_2O$ by XRD and confirmed to be free of $Fe^{3+}$ as deduced by Mössbauer spectrum recorded in the transmission geometry in the constant acceleration mode.

Turning to the synthesis of tavorite-type $LiFeSO_4F$, the solid-state reaction was excluded from this investigation, with efforts focused instead on revisiting the less energy-intensive solvothermal and ionothermal synthesis protocols, owing to the difficulties encountered in routinely reproducing them. We surveyed various parameters, including solvent type, reaction time, and reaction temperature. Equimolar amounts of $FeSO_4{\cdot}H_2O$ and LiF were intimately mixed and placed in a 125 mL Teflon-lined stainless steel autoclave with 30 mL of TTEG ($C_7H_{13}O_4$, Sigma-Aldrich, 99%) or 5 mL of EMI-TFSI depending on the synthesis route. The autoclave was sealed under Ar and placed in a muffle furnace. The temperature was raised to 160 ˚C at 5 ˚C $min^{-1}$ and then to desired temperatures (220-250 ˚C for solvothermal reaction and 280-310 ˚C for ionothermal reaction) at 1 ˚C $min^{-1}$ for a predefined time (12-60 hours). When the reaction was completed, the furnace was cooled down to room temperature. The product was separated by centrifugation, washed several times with acetone or dichloromethane, and dried under vacuum at 50 ˚C overnight prior to being characterized for phase purity and oxidation state of iron.

The corresponding XRD patterns are shown in **Fig. 1 (a)-(b)**. For the solvothermal reaction, phase-pure $LiFeSO_4F$ could not be formed in 24 hours below 250 ˚C because of a sluggish reaction rate, while the formation of $FeSO_4$ impurity can be observed when the temperature was too high. Similar phenomena were also observed in ionothermal syntheses, with tavorite-type $LiFeSO_4F$ only forming in a very narrow temperature range. Improper reaction setting would inevitably lead to $FeSO_4{\cdot}H_2O$ or $FeSO_4$ impurity phases whose characteristic peaks are located at 23.6˚ and 34.1˚, respectively. No $Fe^{3+}$ ion was detected by Mössbauer spectroscopy, implying the high purity of the as-prepared $LiFeSO_4F$ samples. This survey shows that the best experimental condition for producing phase-pure $LiFeSO_4F$ free of $Fe^{3+}$ is to heat the precursors at 230 ˚C for 60 hours in TTEG, or at 305 ˚C for 24 hours in EMI-TFSI. Such conditions were systematically used to prepare single-phased tavorite-type $LiFeSO_4F$ powders to be studied in this paper.

Previous reports have mentioned that $LiFeSO_4F$ could not be synthesized by hydrophilic ionic liquids such as 1-butyl-3-methylimidazolium trifluoromethanesulphonate (bmim-TfO),[1] and the difficulties in maintaining the low water content in highly hydroscopic TTEG. At this stage an obvious extension of our work was to check the impact of the reacting media water content on the progress of the topotactic reaction leading to the formation of $LiFeSO_4F$. $LiFeSO_4F$ syntheses were conducted by i) systematically controlling the water content of both TTEG and EMI-TFSI reacting media using a Metrohm 831 Karl Fischer coulometer (Ionenstrasse, Switzerland), and ii) monitoring the room temperature (25 ˚C) RH of the working place which is geographically dependent and can easily reach more than 80% in certain places (*e.g.* Hong Kong, where most of this work was carried out). In practice, moist Ar gas was bubbled into TTEG to increase its water content from 540 to 3100 ppm according to Karl Fischer measurements. As was anticipated, we were unable to synthesize phase-pure $LiFeSO_4F$ when the solvent water content was increased, specifically at contents greater than 1200 ppm. A significantly reduced reaction rate was observed, which signified the strong impact of water content of the reaction media on the synthesis of $LiFeSO_4F$. This parameter has not adequately captured researchers' attention, which explains why the reported data are limited and inconsistent.

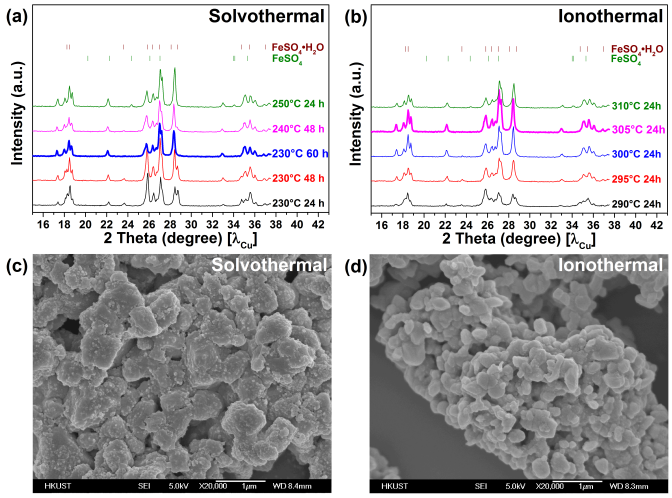


**Fig. 1** XRD screening of synthesis conditions of tavorite-type $LiFeSO_4F$ by **(a)** solvothermal and **(b)** ionothermal methods, and particle morphology of samples synthesized by optimized **(c)** solvothermal and **(d)** ionothermal protocols.

## Electrochemical performance

The electrochemical performance of as-synthesized $LiFeSO_4F$ powders was assessed in both 2025-type coin cells and Swagelok-type cells. To prepare coin cell electrodes, 70 wt% of active material was mixed with 20 wt% of conductive carbon Super P and 10 wt% of polyvinylidene fluoride (PVDF) binder in 1:20 w/w *N*-methyl-2-pyrrolidinone (NMP) solution by planetary ball-milling at 400 rpm for 2 hours. The resultant slurry was cast on Al foils in a room without specific humidity control. To prepare Swagelok cathodes, 80 wt% of $LiFeSO_4F$ and 20 wt% of carbon Super P (denoted hereafter as $LiFeSO_4F$-C) were intimately mixed by ball-milling in Ar. Both type of cells were assembled in an Ar-filled glovebox with $O_2$ and $H_2O$ contents less than 1 ppm, using cast Al foil (coin cell) or composite powders (Swagelok) as the cathode, metallic Li as the anode, 1 M of $LiPF_6$ in ethylene carbonate (EC) and dimethyl carbonate (DMC) (1:1 v/v) as the electrolyte, and Celgard 2325 membrane (coin cell) or two pieces of Whatman GF/D glass fiber (Swagelok) as the separator. Cells were cycled on a LAND CT2001A battery tester (Wuhan, China) or a Mac-Pile system (BioLogic S.A., Claix, France) in galvanostatic mode between 4.5 and 2.2 V vs. Li at 25 ˚C using a current density of C/20.

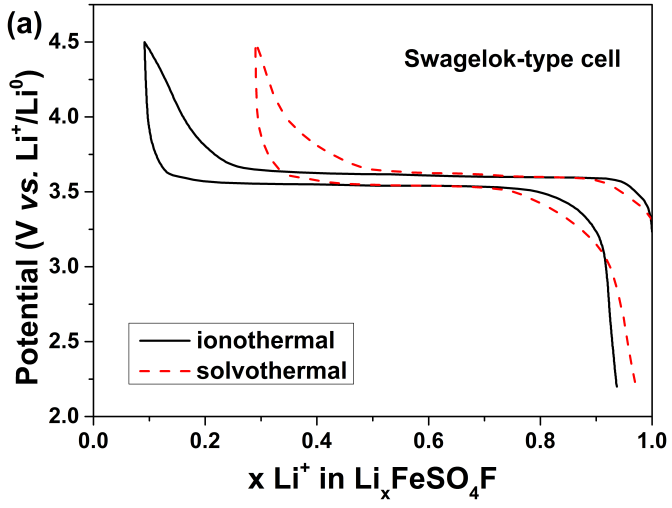


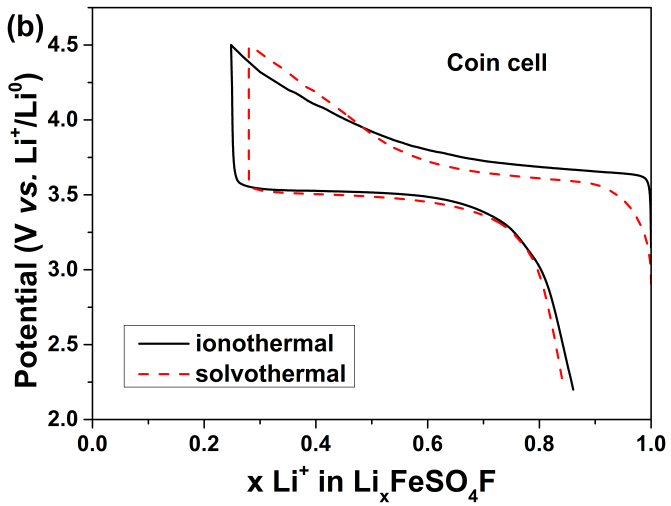


**Fig. 2** First cycle performance of ionothermal (black) and solvothermal (red) samples at a current density of C/20 **(a)** in Swagelok-type cells and **(b)** in coin cells.

**Fig. 2 (a)** compares the performances of LiFeSO4F samples prepared *via* ionothermal and solvothermal routes in Swagelok-type cells. The ionothermally-obtained sample outperforms the solvothermally-prepared sample, which can be well explained from morphology and conductivity perspectives. As compared in **Fig. 1 (c)-(d)**, the as-synthesized ionothermal sample has a much smaller average particle size (~300 nm) than the solvothermal one (~850 nm). Smaller particles lead to a shortened diffusion path for $Li^+$ and to better electrode kinetics in agreement with our experimental results. Another possibility to account for such a difference could be the presence of an EMI-TFSI grafting layer at the surface of $LiFeSO_4F$ which will enhance the ionic conductivity, as previously reported for $LiZnSO_4F$.[12] This would contrast with an ionic blocking thin layer of TTEG at the surface of $LiFeSO_4F$ made in glycol-based media, although such a possibility is therefore quite unlikely given that repeatedly washing the sample yielded no changes in performance.

A similar trend in the electrochemical performance between ionothermal and solvothermal samples was found as expected when the tests were performed using coin cells. In contrast, their poor overall performances (limited reversible capacity, larger polarization) as compared to Swagelok hardware came as a total surprise. It should be noted that the RH was not strictly controlled in the course of coin cell assembly, which further implicates the limited chemical stability of $LiFeSO_4F$ against water.

To shed some light on this issue we decided to study the effect of water on the structural stability of $LiFeSO_4F$ when aged in various RH. Thus we quantitatively mimicked humid environments using saturated salt solutions that are commonly known to produce stable RH at certain temperatures in a closed system.[13-15] $LiFeSO_4F$ powders were left for various amounts of time in desiccators containing $Mg(NO_3)_2$, $NH_4NO_3$, NaCl, and KCl saturated solutions with autogenous equilibrium RH of 53%, 62%, 75%, and 85%, respectively at 25 ˚C as determined by a hygrometer within an accuracy of ±1%. **Fig. 3** shows the evolution of the XRD patterns of powders left for 36 hours under different RH. Strikingly, we noted a rapid disappearance of the Bragg peaks pertaining to the tavorite phase with increasing humidity so that by 75% RH $LiFeSO_4F$ has totally decomposed. At this stage it is worth mentioning that a significantly accelerated decomposition rate was found for ball-milled $LiFeSO_4F$-C electrodes due to their highly divided nature. XRD patterns of the fully transformed samples indicate the coexistence of multiple hydrated sulfate phases ($FeSO_4 \cdot nH_2O$, with n =1, 4, and 7). Their relative amounts, quantified by Rietveld

refinement[16] performed with the FullProf suite[17] (**Fig. S2**), were found to depend upon the exposure time to humidity, with the n = 7 member dominating at longer exposures.

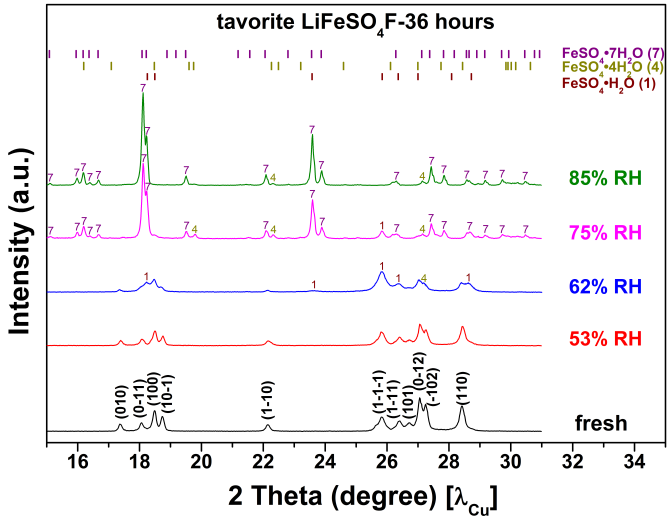


**Fig. 3** XRD patterns of tavorite-type $LiFeSO_4F$ powders left in humid environment at 25 °C for 36 hours as a function of RH.

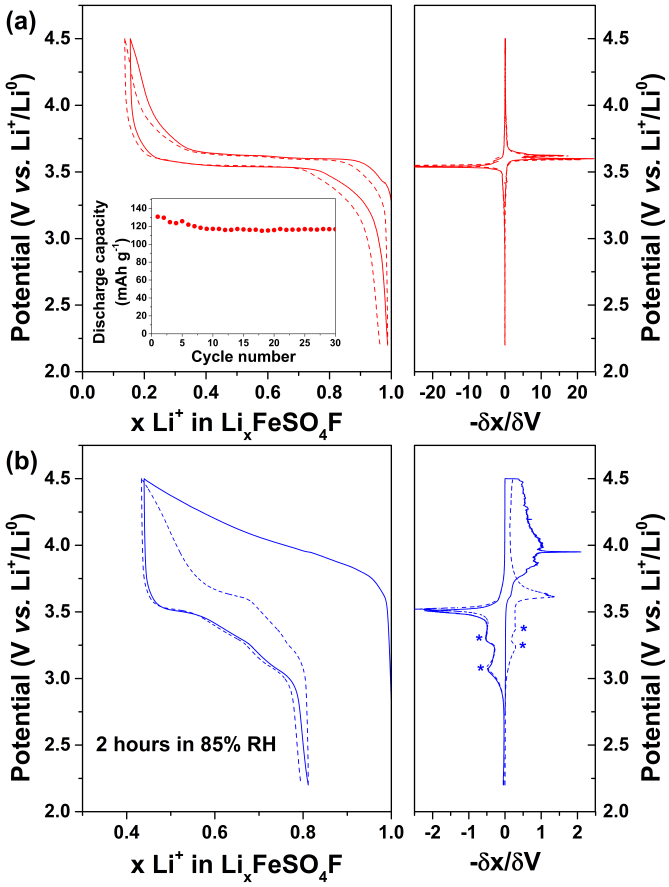


**Fig. 4** Electrochemical behaviors (left) of $LiFeSO_4F$ electrode in contact with 85% RH at 25 °C for **(a)** 0 hour and **(b)** 2 hours and their corresponding differential capacity curves (right). Inset shows cycling performance of fresh $LiFeSO_4F$ electrode.

Swagelok-type cells containing $LiFeSO_4F$ samples aged under various RH were assembled and their performances are shown in **Fig. 4**. For fresh composite powders without any contact to moisture, the voltage composition curve and its accompanying derivative in **Fig. 4 (a)** indicate, in agreement with the literature, a 3.6 V *vs.* Li plateau which corresponds to the reversible uptake of ~0.85 $Li^+$. This drastically contrasts with the sloping voltage profile recorded for $LiFeSO_4F$-C powders left in 85% RH for 2 hours in **Fig. 4 (b)**. Upon cycling, the derivative curve (**Fig. 4 (b)** right) shows the onset of two additional redox pairs located near 3.3 and 3.1 V. Whether purely coincidental or not, such peaks were found to correspond to the electrochemical signatures of tavorite-type (Li)$FeSO_4OH$ *vs.* Li,[18] hence suggesting the *in situ* formation of the electrochemically active (Li)$FeSO_4OH$ during the cycling of $LiFeSO_4F$ samples exposed to highly humid environment. This does not come as a full surprise since both $OH^-$ and $F^-$ species share various similarities and can co-exist in minerals such as triplite $(Mg,Fe)_2(PO_4)(F,OH)$, creedite $Ca_3Al_2SO_4(F,OH)\cdot 2H_2O$, and norbergite $Mg_3(SiO_4)(F,OH)_2$. Nevertheless, the mechanism of this transformation calls for better understanding of the stability of the tavorite $LiFeSO_4F$ phase.

To grasp further insight into the *in situ* formation of (Li)$FeSO_4OH$ and test whether $F^-$ was involved in this process we performed a similar experiment using a $F^-$-free sulfate electrode exposed to the same degree of RH (85%) as previously described for $LiFeSO_4F$. We selected $FeSO_4$ since we experienced its progressive capture of water when placed in high RH environment. **Fig. 5** shows the electrochemical performance of electrodes that were made out of this sample and tested in coin cells. The cells were started on charge. The voltage increased continuously up to 4.5 V. In contrast, the discharge curve shows a step-wise profile with the appearance of the 3.3 and 3.1 V plateaus corresponding to (Li)$FeSO_4OH$. The subsequent curves mirror nicely the first discharge but drastically deviate from the first charge, suggesting that the electrode has undergone major structural/compositional change during the first charge. Once this transformation is done, the electrode shows a sustained reversibility of ~100 mAh $g^{-1}$ while maintaining the characteristics of (Li)$FeSO_4OH$, hence providing an irrefutable proof for its *in situ* formation. It is worth noting that similar charge and discharge profiles were also observed by two other groups,[19,20] but neither of them checked the moisture sensitivity issue nor reported the signature of (Li)$FeSO_4OH$ in their voltage curves.

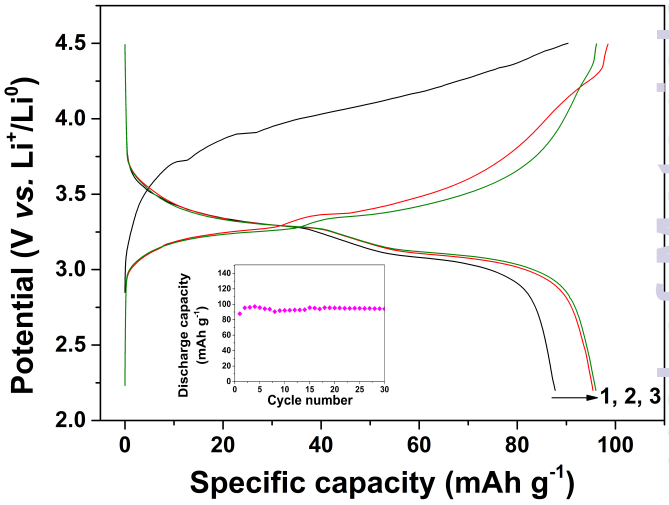


**Fig. 5** First three cycles of moisture affected $FeSO_4$. The inset shows the discharge capacity of first 30 cycles.

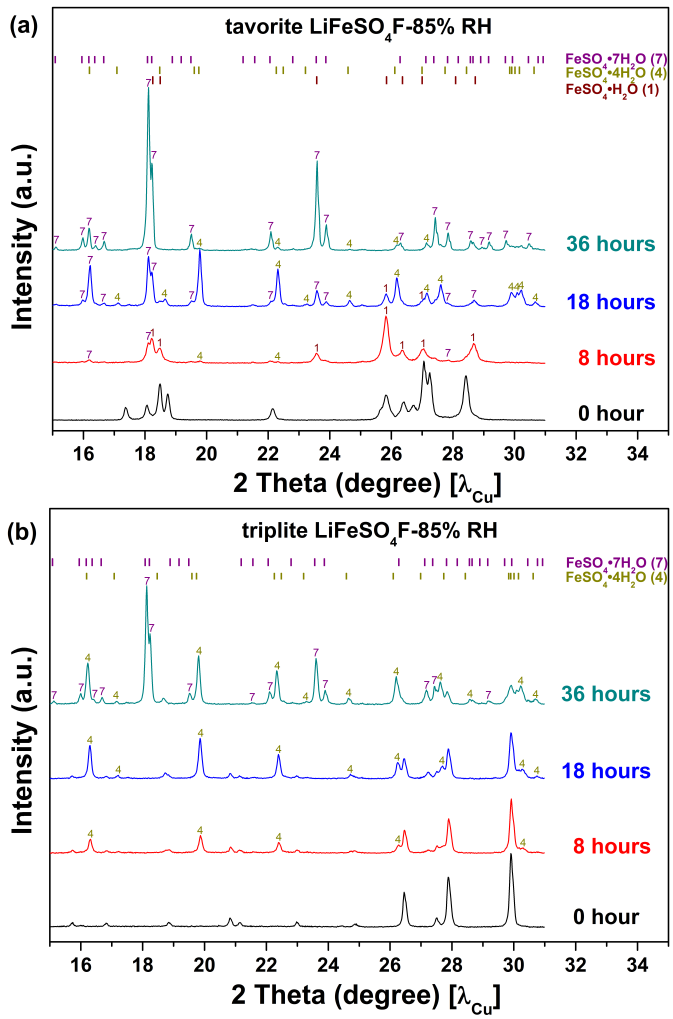


**Fig. 6** XRD patterns of **(a)** tavorite and **(b)** triplite $LiFeSO_4F$ powders left in 85% RH at 25 ˚C as a function of time.

The aforementioned XRD and electrochemical studies strongly indicate that a pre-requisite for achieving optimized performance with tavorite-type $LiFeSO_4F$ is to operate in a dry reaction media (water content < 1000 ppm). At this stage, a legitimate question is whether the triplite polymorph, which offers a 300 mV advantage in operating potential, is as moisture sensitive as its tavorite counterpart. We checked this issue by adopting the same methodology and found a similar behavior with a lower degradation rate as shown by the XRD patterns collected as a function of time in 85% RH. Rietveld refinements indicate that both compounds transforms into successive hydrated iron sulfate phases. Note that for 85% (**Fig. 6**) and 62% RH (**Fig. S3**), the tavorite phase fully disappeared after 8 and 200 hours, respectively while the triplite phase was still present. This is indicative of a better resistance of the triplite phase against moisture, in good agreement with calorimetry measurements which have shown that among the two polymorphs the triplite phase is thermodynamically more stable.[21] We also generalized our study to other Li(Na)-based sulfate phases ($LiFeSO_4OH$,[22] $FeSO_4OH$,[18] $Fe_2O(SO_4)_2$,[23] $Li_2Fe(SO_4)_2$ polymorphs,[24,25] and $Na_2Fe_2(SO_4)_3$[26]) (**Fig. 7**). Apart from the $Fe_2O(SO_4)_2$ oxysulfate, the others were shown to react with water as well with different degrees of severity depending upon their structure and state of division, thus leading to the general conclusion that moisture sensitivity is inherent to sulfate-based electrodes. This does not come as a surprise as sulfates are known to be soluble in water,[27] because oxygen atoms in both $SO_4^{2-}$ and $H_2O$ have comparable Lewis basicity (~0.17 v.u.), which is for instance not the case for phosphates (~0.25 v.u.). The insolubility of the oxysulfate $Fe_2O(SO_4)_2$ may therefore be explained by the presence of an oxygen atom that does not belong to any sulfate group, which therefore presents a different Lewis basicity and limits its moisture sensitivity.

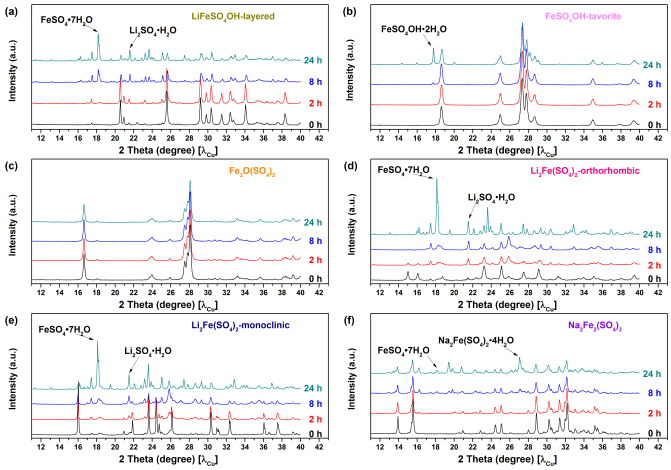


**Fig. 7** Moisture sensitivity test of sulfate-based cathode materials, including **(a)** $LiFeSO_4OH$-layered, **(b)** $FeSO_4OH$-tavorite, **(c)** $Fe_2O(SO_4)_2$, **(d)** $Li_2Fe(SO_4)_2$-orthorhombic, **(e)** $Li_2Fe(SO_4)_2$-monoclinic, and **(f)** $Na_2Fe_2(SO_4)_3$. Powders were placed in a desiccator with 85% RH for 2 hours (red), 8 hours (blue), and 24 hours (dark cyan) and compared with pristine ones (black). New phases are identified with arrows.

## Discussion and conclusion

We have reported the extreme sensitivity of $LiFeSO_4F$ and sulfates in general to moisture, and revealed the feasibility to electrochemically trigger the *in situ* formation of (Li)$FeSO_4OH$. An understanding of the mechanism(s) by which such compounds react with water is a critical step towards proposing solutions for their practical use as electrodes. Similarly, identifying the reacting steps involved in the formation of (Li)$FeSO_4OH$ could enable us to prepare other novel materials. Both of these points are discussed below.

Let's first turn to the synthesis of tavorite $LiFeSO_4F$ that relies on a topotactic reaction enlisting a *quasi*-equilibrium state between $FeSO_4{\cdot}H_2O$ and $LiFeSO_4F$ (***Eq. 1***). When $H_2O$ is present in great excess, according to Le Chatelier's principle, the backward reaction (***Eq. 2***) is preferred with LiF precipitated as dead weight. In addition, Mitchell has discovered that when the RH is higher than 65%, $FeSO_4{\cdot}H_2O$ will spontaneously absorb water at 25 ˚C (***Eqs. 3*** and ***4***) to respectively form $FeSO_4{\cdot}4H_2O$ and $FeSO_4{\cdot}7H_2O$.[28] Thus, the continuous consumption of $FeSO_4{\cdot}H_2O$ further promotes the spinodal decomposition of $LiFeSO_4F$, as illustrated in **Fig. 8**. Lastly, based on the tiny amount of $Li_2SO_4{\cdot}H_2O$ observed among the decomposition products, the feasibility of having a competing degradation path in accordance with ***Eq. 5*** cannot be fully disregarded.

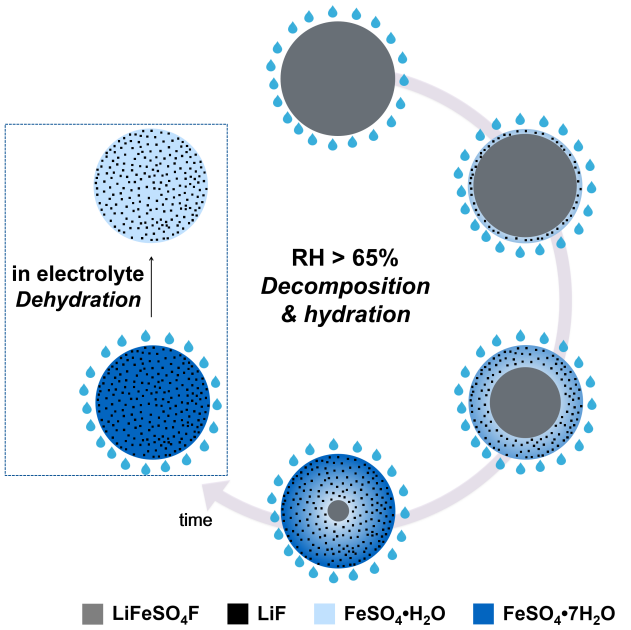


**Fig. 8** Schematic illustration of the decomposition & hydration processes of $LiFeSO_4F$ in humid environment (RH > 65%), and the dehydration of $FeSO_4 \cdot 7H_2O$ in the electrolyte.

When electrodes made out of these water-bearing $LiFeSO_4F$ materials are placed in contact with electrolyte, $H_2O$ molecules released from i) surface adsorption and ii) $FeSO_4 \cdot 4H_2O$ and $FeSO_4 \cdot 7H_2O$ dehydration will induce $LiPF_6$ decomposition and HF formation.[29,30] This corrosive species will attack the electrode, leading to metal dissolution and performance degradation. Although switching to $LiClO_4$ salt may prevent HF formation, the degradation of the cathode material at highly humid environment is always irreversible. A detailed analysis on water content is provided in the supporting information (**Fig. S4**).

$$LiFeSO_4F + H_2O \rightarrow FeSO_4 \cdot H_2O + LiF \quad (2)$$

$$FeSO_4 \cdot H_2O + 3H_2O \underset{\text{electrolyte}}{\overset{RH>65\%}{\rightleftharpoons}} FeSO_4 \cdot 4H_2O \quad (3)$$

$$FeSO_4 \cdot 4H_2O + 3H_2O \underset{\text{electrolyte}}{\overset{RH>65\%}{\rightleftharpoons}} FeSO_4 \cdot 7H_2O \quad (4)$$

$$2LiFeSO_4F + 2H_2O \rightarrow Li_2SO_4 \cdot H_2O + FeSO_4 \cdot H_2O + FeF_2 \quad (5)$$

From this study, two RH domains appear critical for handling $LiFeSO_4F$: for RH ≤ 50% spinodal decomposition is retarded, whereas decomposition occurs at an exceedingly fast rate for RH ≥ 65%. Therefore, the RH should be strictly controlled when processing $LiFeSO_4F$ in order to retain good electrode performance. Alternatively, coating a protective layer on particle surfaces may also improve moisture resistivity. Hence, it does not come as a surprise that enrobing the powder by a layer of conductive polymer poly-3,4-ethylene-dioxythiophene (PEDOT) has led to enhanced performance for this material.[9] We performed preliminary polymer coating on tavorite $LiFeSO_4F$, and confirmed, using a similar test protocol a lower decomposition rate compared to the pristine sample. Another option is to incorporate the tavorite $LiFeSO_4F$ phase with carbonaceous materials, such as hierarchical graphene-nanostructuring[31] and low temperature carbon coating.[32] We effectively experienced that these treatments can help mitigate the impact of moisture.

Lastly, to shed light on the formation of the $F^-$-free (Li)$FeSO_4OH$, we examined the role of $H_2O$ and here we provide a possible interpretation. Introduction of $H_2O$ to non-aqueous electrolyte worsens the durability of the system,[33-37] leading to the formation of intermediate nucleophile species ($OH^-$, $O^{2-}$, *etc.*) upon oxidation. Being strong Lewis bases, these species may oxidize iron, ending up with the formation of $FeSO_4OH$. It is worth mentioning that researchers on nuclear chemistry also observed oxidation of $Fe^{2+}$ by nucleophile species through gamma-radiolysis of iron sulfate hydrates.[38-40] In a controlled experiment, dry $FeSO_4 \cdot H_2O$ powders with 20 wt% of carbon were directly assembled in Swagelok-type cell to avoid any free $H_2O$, and no activity was recorded (**Fig. S5**). To confirm the inertness of $FeSO_4 \cdot H_2O$, we also attempted chemical oxidation by excess amount of $NO_2BF_4$ (Sigma-Aldrich, ≥95%) in acetonitrile. The recovered compound was placed in a Swagelok-type cell but showed no electrochemical activity. Thus, we claim the vital importance of having free $H_2O$ species in the formation of $FeSO_4OH$. However, we are unable to record good reflection peaks of crystalline (Li)$FeSO_4OH$ phase at the end of (dis)charge, but mainly see bulk $FeSO_4 \cdot H_2O$ peaks, implying that the electrochemically active species is most probably amorphous. This situation is somewhat similar to what was encountered by Guyomard and co-workers on the ageing of $LiFePO_4$ in the presence of moisture for T > 100 °C, where the authors have reported the growth of an X-ray amorphous $LiFePO_4OH$ phase on the surface of the aged $LiFePO_4$.[41]

To gain better insight into the local iron environments in tavorite-type $LiFeSO_4F$ during its reaction with moisture and its phase evolution in an electrochemical cell, room temperature Mössbauer spectroscopy was conducted. Refinement details are provided in the Electronic Supplementary Information. The spectra of **(a)** fresh $LiFeSO_4F$-C, **(b)** aged $LiFeSO_4F$-C in 85% RH for 4 hours, as well as **(c)** collected discharge product of the aged $LiFeSO_4F$-C after 40 cycles are fitted and compared with **(d)** literature data of $LiFeSO_4OH$ in **Fig. 9**. The pristine $LiFeSO_4F$-C sample has two distinct $Fe^{2+}$ crystallographic sites, in good accordance with previous measurements.[42,43] After 4-hour exposure in 85% RH, ~20% of $Fe^{3+}$ from accelerated moisture oxidation is observed, demonstrating the necessity to use ascorbic acid to remove $Fe^{3+}$ ions during material preparation as we mentioned previously. The remaining 80% of $Fe^{2+}$ can be fitted by a single doublet corresponding to $Fe^{II}O_4(OH_2)_2$ octahedra in $FeSO_4 \cdot H_2O$. Now turning to the electrochemically cycled sample recovered at the end of discharge, a new doublet (dark red line in **Fig. 9 (c)**) accounting for 33% of the Fe signal and having similar IS and QS as $Fe^{2+}$ site in tavorite-type $LiFeSO_4OH$ has been recorded.[44] Moreover, in spite of the drastic change in the Fe local environment through oxidation, it is worth mentioning that the $Fe^{3+}$ signal corresponding to the $Fe^{3+}$ impurity has slightly broadened due a distortion of its electronic charge caused by neighboring species, but its amount has not changed. This suggests that the $Fe^{3+}$ bearing impurity whose origin is not fully identified does not seriously interfere the investigation of the (Li)$FeSO_4OH$-like phase.

Here, we propose a core-shell model to estimate chemical compositions of the moisture affected $LiFeSO_4F$. Having noticed that $FeSO_4 \cdot H_2O$ is the only stable hydrated phase in the electrolyte, if we assume $FeSO_4 \cdot H_2O$ particles spherical, the thickness of the electrochemically active $FeSO_4 \cdot H_2O$ shell, taking into account the $Fe^{3+}$ impurities, is calculated as 22% of the particle radius, which is rational for the core-shell model we have proposed here. By the end of first charge, while the inner $FeSO_4 \cdot H_2O$ (core) remains unchanged, surface $FeSO_4 \cdot H_2O$ (shell) is readily oxidized by nucleophile species to form a new $Fe^{3+}$ compound, which is then reduced in discharge. An uptake of 0.35 $Li^+$ from the discharged sample is in good agreement with the 33% of $LiFeSO_4OH$ sites calculated from the Mössbauer spectrum. Therefore, although the electrochemically active species is probably X-ray amorphous, we may still deduce its chemical nature being tavorite-type



 

(Li)$FeSO_4OH$ from both differential capacity curves and Mössbauer spectra.

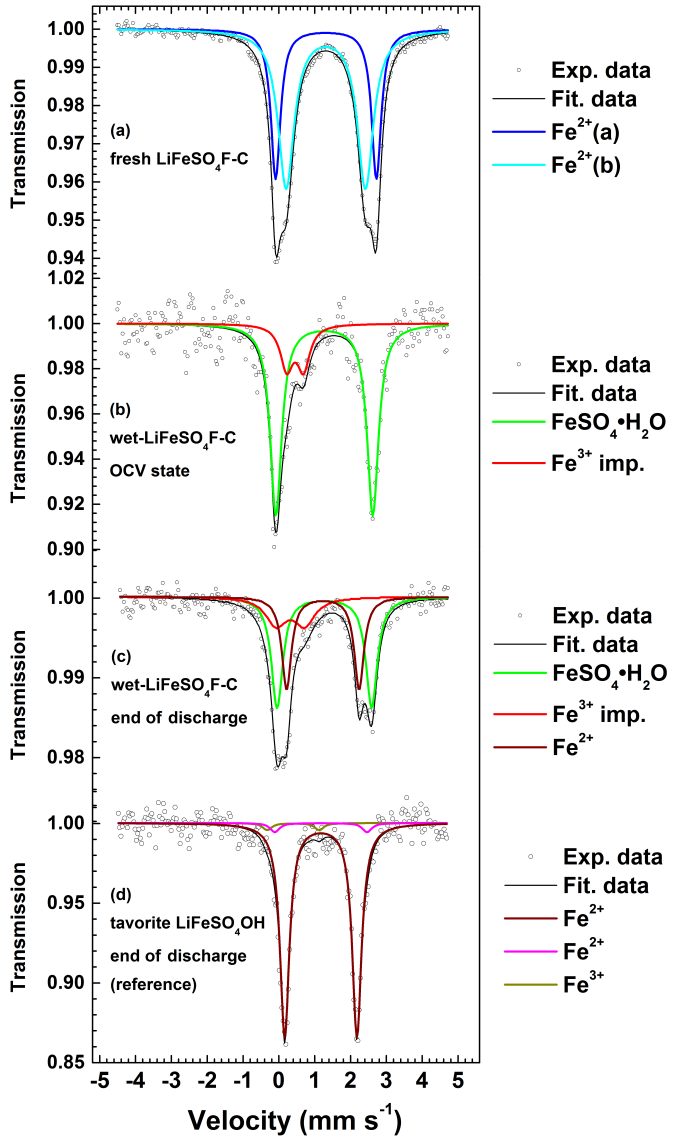


**Fig. 9** Mössbauer spectra of **(a)** fresh $LiFeSO_4F$-C, **(b)** aged $LiFeSO_4F$-C in 85% RH for 2 hours, **(c)** discharge product of the aged $LiFeSO_4F$-C after 40 cycles, and **(d)** reference $LiFeSO_4OH$-C at discharge state.

In conclusion, we have reported reproducible production of phase-pure tavorite $LiFeSO_4F$ using both solvothermal and ionothermal methods, and demonstrated *via* XRD that the phase is extremely sensitive to moisture. While the material remains intact for several months when the RH is below 50%, there is a full and rapid decomposition of $LiFeSO_4F$ into $FeSO_4{\cdot}nH_2O$ (n = 1, 4, 7) and LiF in highly humid environment (>62% RH at 25 ˚C). Special cares will have to be exercised in processing sulfates for large-scale applications. Water sources along the synthesis and processing of $LiFeSO_4F$ electrodes should be maximally eliminated. Nevertheless, such manufacturing difficulties can be mitigated *via* the use of surface modified particles with PEDOT, carbon coating, hierarchical nanostructuring, or other techniques that remain to be designed. This moisture reactivity, including both decomposition and hydration reactions, is applicable to sulfate-based electrode materials in general; the only exception we found is the oxysulfate phase, $Fe_2O(SO_4)_2$, which does not react with moisture. Lastly, the feasibility to electrochemically form (Li)$FeSO_4OH$ in an in situ way, offers another approach to stabilizing metastable phases that has been poorly explored to date.

## Acknowledgements

This work was funded by the Hong Kong Research Grant Council under RGC-GRF 611213. The authors thank C. Cheung (HKUST) for taking XRD measurements and J. Kurzman for his critical reading of the paper. L.Z. acknowledges HKUST for his Postgraduate Studentships. Fruitful discussions with H. Xu, E. McCalla, and A. Grimaud are gratefully appreciated. J.M.T. acknowledges the Institute for Advanced Study of HKUST for partly sponsoring his professorship. G.H.C. acknowledges the Research Excellence Fund from School of Engineering, HKUST, SBI11EG13. The authors thank M. Sun, B. Zhang, L. Lander, and L. Lutz for preparing sulfate-based samples for the humidity test.

## Notes and references

1 N. Recham, J. N. Chotard, L. Dupont, C. Delacourt, W. Walker, M. Armand and J. M. Tarascon, *Nature Mater.*, 2010, **9**, 68–74.
2 P. Barpanda, M. Ati, B. C. Melot, G. Rousse, J. N. Chotard, M. L. Doublet, M. T. Sougrati, S. A. Corr, J. C. Jumas and J. M. Tarascon, *Nature Mater.*, 2011, **10**, 772–779.
3 L. Liu, B. Zhang and X.-J. Huang, *Prog Nat Sci*, 2011, **21**, 211–215.
4 M. Ati, B. C. Melot, J. N. Chotard, G. Rousse, M. Reynaud and J. M. Tarascon, *Electrochem. Commun.*, 2011, **13**, 1280–1283.
5 M. Ati, M. T. Sougrati, N. Recham, P. Barpanda, J. B. Leriche, M. Courty, M. Armand, J. C. Jumas and J. M. Tarascon, *J. Electrochem. Soc.*, 2010, **157**, A1007–A1015.
6 R. Tripathi, T. N. Ramesh, B. L. Ellis and L. F. Nazar, *Angew. Chem. Int. Ed.*, 2010, **49**, 8738–8742.
7 R. Tripathi, G. Popov, B. L. Ellis, A. Huq and L. F. Nazar, *Energy Environ. Sci.*, 2012, **5**, 6238–6246.
8 S. L. Yang, L. P. Wang, R. G. Ma, Z. G. Lu, L. J. Xi, M. J. Hu, Y. C. Dong and C. Y. Chung, *J. Electrochem. Soc.*, 2013, **160**, A3072–A3076.
9 A. Sobkowiak, M. R. Roberts, R. Younesi, T. Ericsson, L. Haggstrom, C.-W. Tai, A. M. Andersson, K. Edström, T. Gustafsson and F. Björefors, *Chem. Mater.*, 2013, **25**, 3020–3029.
10 C. Masquelier and L. Croguennec, *Chem. Rev.*, 2013, **113**, 6552–6591.
11 G. Rousse and J. M. Tarascon, *Chem. Mater.*, 2014, **26**, 394–406.
12 P. Barpanda, R. Dedryvère, M. Deschamps, C. Delacourt, M. Reynaud, A. Yamada and J. M. Tarascon, *J. Solid State Electrochem.*, 2011, **16**, 1743–1751.
13 P. W. Winston and D. H. Bates, *Ecology*, 1960, **41**, 232–237.
14 L. Greenspan, *J. Res. Nat. Stand. Sec. A*, 1977, **81A**, 89–96.
15 A. Wexler and S. Hasegawa, *J. Res. Nat. Stand. Sec. A*, 1954, **53**, 19–26.
16 H. M. Rietveld, *J. Appl. Cryst.*, 1969, **2**, 65–71.
17 J. Rodríguez-Carvajal, *Physica B*, 1993, **192**, 55–69.
18 M. A. Reddy, V. Pralong, V. Caignaert, U. V. Varadaraju and B. Raveau, *Electrochem. Commun.*, 2009, **11**, 1807–1810.
19 S.-W. Kim, K.-W. Nam, D.-H. Seo, J. Hong, H. Kim and H. Gwon, *Nano Today*, 2012, **7**, 168–173.
20 X.-M. Liu, S.-L. Zhang, M. Yang, X.-Z. Liao, H. Yang, X.-D. Shen and Z.-F. Ma, *Chem. Commun.*, 2014, **50**, 15247–15250.

21 A. V. Radha, J. D. Furman, M. Ati, B. C. Melot, J. M. Tarascon and A. Navrotsky, *J. Mater. Chem.*, 2012, **22**, 24446–24452.
22 C. V. Subban, M. Ati, G. Rousse, A. M. Abakumov, G. Van Tendeloo, R. Janot and J. M. Tarascon, *J. Am. Chem. Soc.*, 2013, **135**, 3653–3661.
23 M. Sun, G. Rousse, A. M. Abakumov, G. Van Tendeloo, M. T. Sougrati, M. Courty, M.-L. Doublet and J. M. Tarascon, *J. Am. Chem. Soc.*, 2014, **136**, 12658–12666.
24 L. Lander, M. Reynaud, G. Rousse, M. T. Sougrati, C. Laberty-Robert, R. J. Messinger, M. Deschamps and J. M. Tarascon, *Chem. Mater.*, 2014, **26**, 4178–4189.
25 M. Reynaud, M. Ati, B. C. Melot, M. T. Sougrati, G. Rousse, J.-N. Chotard and J. M. Tarascon, *Electrochem. Commun.*, 2012, **21**, 77–80.
26 P. Barpanda, G. Oyama, S.-I. Nishimura, S.-C. Chung and A. Yamada, *Nat. Commun.*, 2014, **5**, 4358.
27 I. D. Brown, *Struct Bond*, 2014, **158**, 11–58.
28 A. G. Mitchell, *J. Pharm. Pharmacol.*, 1984, **36**, 506–510.
29 S. F. Lux, I. T. Lucas, E. Pollak, S. Passerini, M. Winter and R. Kostecki, *Electrochem. Commun.*, 2012, **14**, 47–50.
30 D. Aurbach, *J. Power Sources*, 2000, **89**, 206–218.
31 Y. Meng, S. Zhang and C. Deng, *J. Mater. Chem. A*, 2015, **3**, 4484–4492.
32 A. Ponrouch, A. R. Goñi, M. T. Sougrati, M. Ati, J. M. Tarascon, J. Nava-Avendaño and M. R. Palacín, *Energy Environ. Sci.*, 2013, **6**, 3363–3371.
33 D. Aurbach and H. Gottlieb, *Electrochim. Acta*, 1989, **34**, 141–156.
34 F. Joho and P. Novak, *Electrochim. Acta*, 2000, **45**, 3589–3599.
35 W. Li and B. L. Lucht, *Electrochem. Solid State Lett.*, 2007, **10**, A115–A117.
36 D. Aurbach, I. Weissman, A. Zaban and P. Dan, *Electrochim. Acta*, 1999, **45**, 1135–1140.
37 M. Koltypin, D. Aurbach, L. F. Nazar and B. Ellis, *Electrochem. Solid State Lett.*, 2007, **10**, A40–A44.
38 J. Meyers, J. Ladriere, M. Chavee and D. Apers, *J. Phys. Colloques*, 1976, **37**, 905–908.
39 N. Sakai, H. Sekizawa and K. Ono, *J. Inorg. Nucl. Chem.*, 1981, **43**, 1731–1734.
40 J. Ladriere, N. Beckris and D. Apers, *Hyperfine Interact.*, 1992, **70**, 1245–1248.
41 M. Cuisinier, J.-F. Martin, N. Dupré, R. Kanno and D. Guyomard, *J. Mater. Chem.*, 2011, **21**, 18575–18583.
42 A. Sobkowiak, T. Ericsson, K. Edström, T. Gustafsson, F. Björefors and L. Häggström, *Hyperfine Interact.*, 2013, **226**, 229–236.
43 B. C. Melot, G. Rousse, J. N. Chotard, M. Ati, J. Rodríguez-Carvajal, M. C. Kemei and J. M. Tarascon, *Chem. Mater.*, 2011, **23**, 2922–2930.
44 M. Ati, M. T. Sougrati, G. Rousse, N. Recham, M. L. Doublet, J. C. Jumas and J. M. Tarascon, *Chem. Mater.*, 2012, **24**, 1472–1485.